Electronic Supplementary Information (ESI):
A microfluidic platform for probing small artery structure and function

Axel Günther, Sanjesh Yasotharan, Andrei Vagaon, Conrad Lochovsky, Sascha Pinto, Jingli Yang, Calvin Lau, Julia Voigtlaender-Bolz, Steffen-Sebastian Bolz

Supplementary Text, Supplementary Figures S1–S3,
Supplementary Videos S4-S6, Supplementary References

Microfluidic device design and fabrication

Computer-aided design (CAD) drawings of microfluidic channel networks were developed using the software AutoCAD (Autodesk, Inc., San Rafael, CA) and photo-plotted onto transparency masks (resolution: 20,000 dpi, CAD/ART Services, Inc., Bandon, OR), see Fig. S1. Microfluidic devices were designed and fabricated using soft lithography[1, 2] in the elastomeric substrate material poly-(dimethylsiloxane) (PDMS). Briefly, masters with a final feature height of 150±2µm that was verified by optical profilometry (Wyko model NT1100 Optical Profiling System, Veeco Instruments, Camarillo, CA) were fabricated by spin-coating and subsequently pre-baking two consecutive layers of SU-8 2050 negative photoresist (Microchem, Newton, MA) at 1750rpm on top of a seed layer of SU-8 25 that was spun at 2000 rpm. The transparent sections of a laser plotted transparency mask were selectively exposed to UV light (intensity: 220 mJ/cm^2, wavelength: 365nm, model 200 Mask Aligner, Optical Associates International, San Jose, CA), and subsequently developed (SU-8 developer, Microchem Corp., Newton, MA) and baked. Poly-(dimethylsiloxane) (Sylgard 184 Elastomer Kit, Dow-Corning, Midland, MI) was molded on top of the obtained master, was cured, peeled off, cut to either match the footprint of a 75 mm × 25 mm × 1 mm microscope slide (VWR Scientific, West Chester, PA) or of a 60 mm × 24 mm × 130 µm cover slip (No. 1, Corning Inc, Corning, NY), both treated with an oxygen plasma (Expanded Plasma Cleaner, Harrick Plasma, Ithaca, NY) and then bonded to the glass substrate. The completed device was fluidically connected to the outside world using precut, deburred and passivated stainless steel pins (length 12.5mm, type 304 stainless steel 23 gauge pins, New England Small Tube Corp., Litchfield, NH) as well as polymer tubing (Tygon, outer diameter 0.06" and 1/8", Cole-Parmer, Montreal, QC, and Upchurch Scientific, Oak Harbor, WA). All other specialty fluidic connections (leur locks, ferrules and nuts) were obtained from Upchurch Scientific.

Figure S1 shows the detailed layout of the photomask that was used to fabricate the device shown in Fig. 2a. Heating and temperature sensing are integrated so that the physiological temperature can be locally applied at the inspection area of the microfluidic device. A sapphire disk 25 mm in diameter and 1 mm in thickness (Brighten Optics, Richmond, BC, Canada) was embedded on top of the second PDMS layer. Sapphire has a thermal conductivity (41.9W•m^{-1}K^{-1}) that is two hundred times greater than the one of PDMS and forty times greater than the one of borosilicate glass. As a result, the heat generated by a thermoelectric (TE) element was uniformly distributed in the horizontal direction. The TE element and a thermistor were attached to the sapphire disk using thermally conductive epoxy. A chip-external electric PID controller adjusted the heating power such that the artery inspection area was kept at physiological temperature. After connecting the fluidic inlet and outlet lines, the device was placed on the stage of an inverted microscope. Fluid lines were connected to automated syringe pumps and the respective pressures were hydrostatically applied at the outlets.

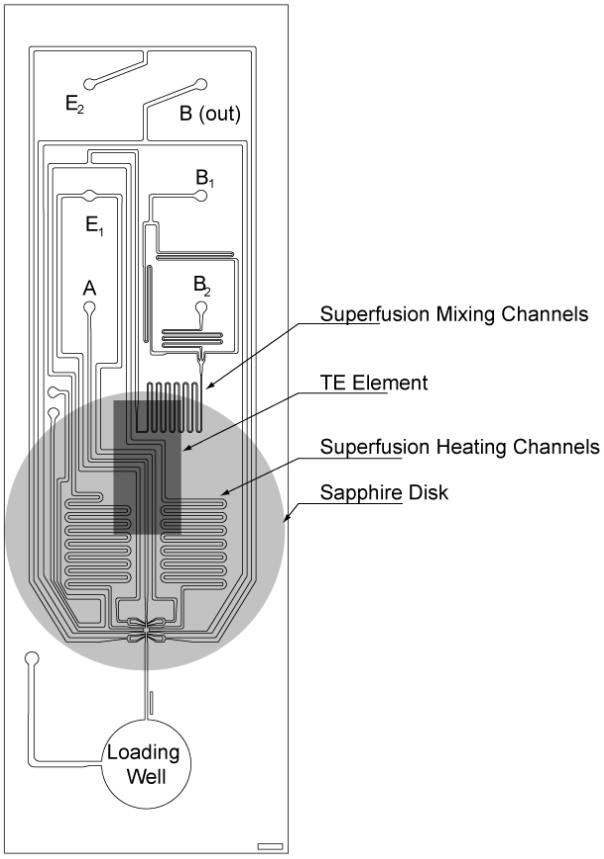

Fig. S1. Transparency mask layout for microfluidic device establishing a homogeneous abluminal microenvironment. The design has a footprint of 25mm × 75mm. The scale bar is 10 mm long. The device incorporates a sapphire disk and thermoelectric (TE) element for consistently maintaining physiological temperature at the artery inspection area.

Automated superfusion and dose-response measurement

Figure S2 shows photographs of the experimental setup that consisted of an upright stereoscopic microscope used for loading small artery segments onto the chip. An inverted bright-field/fluorescence microscope in combination with an intensified CCD camera and automated syringe pumps was used for determining the artery tone. The superfusion flow of MOPS buffer was applied to the device by inserting two 10 mL syringes into separate, computer-controlled Milliliter Syringe Pump Modules (Harvard Apparatus, Holliston, MA) that were operated at a constant total flow rate (4 mL/h in the homogeneous case, 2×2mL/h in the heterogeneous case). The syringes were connected to the microchannels $\mathbf{B_1}$ and $\mathbf{B_2}$ of the microfluidic device. The SMCs on the abluminal side of the vessel were exposed to stepwise changes in the PE concentration while digital bright-field images of the artery segment were recorded using a

Electronic Supplementary Information (ESI):
A microfluidic platform for probing small artery structure and function

Axel Günther, Sanjesh Yasotharan, Andrei Vagaon, Conrad Lochovsky, Sascha Pinto, Jingli Yang, Calvin Lau, Julia Voigtlaender-Bolz, Steffen-Sebastian Bolz

cooled and intensified CCD camera (Retiga 2000R, QImaging, Surrey, BC).

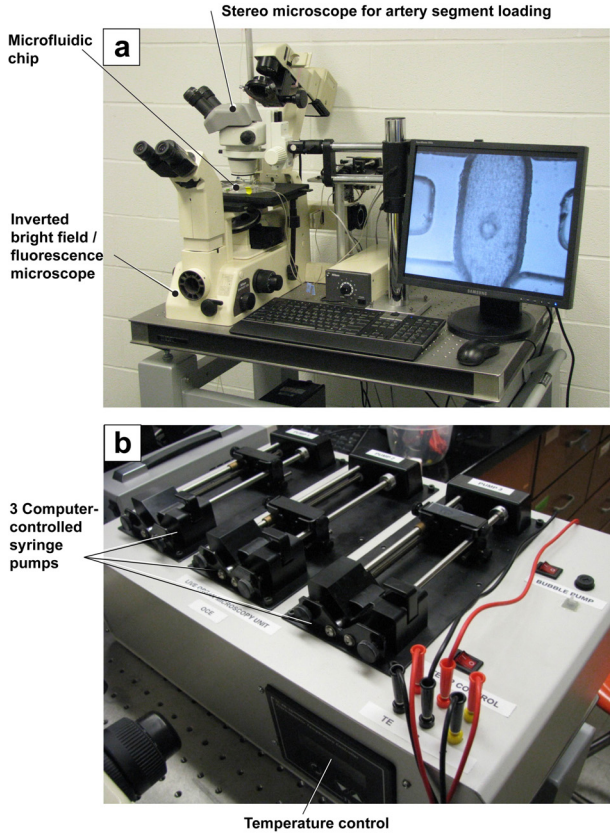

Fig. S2. (a) Photograph of experimental setup consisting of a top-mounted stereoscopic microscope (model SMZ645, Nikon) for manual loading of artery segments combined with an inverted bright field/fluorescence microscope (model diaphot 300, Nikon) for functional assessment. (b) Integrated temperature and perfusion/superfusion flow control unit containing three computer-controlled syringe pumps (Milliliter syringe pump module, Harvard Apparatus, Holliston, MA) as well as a PID controller for establishing physiological temperature in the artery inspection section of the microfluidic device.

A time-dependent dose-response curve was obtained and vascular tone was measured using a custom Matlab (The Mathworks, Inc, Natick, MA) computer program that captured and analyzed the images by detecting the change in image contrast attributed to the artery inner and outer wall surfaces. The computer-controlled pumps were used to alter the drug concentration in the superfusion channel **B** by controlling the individual flow rates of a 3µmol PE in MOPS solution, $\mathbf{Q_{B1}}$, and a MOPS only solution, $\mathbf{Q_{B2}}$, while keeping the total flow rate at 4mL/h For the PE dose-response curve, 5 concentrations between 0.3µmol and 3µmol (specifically, 0.3µmol, 0.9µmol, 1.5µmol, 2.1µmol and 3µmol) were applied in the superfusing stream during 3 min increments. Acetylcholine (Ach) experiments were conducted by initially pre-constricting the artery segment with 1µmol PE followed by application of increasing concentrations of ACh at 3 min intervals. Arterial diameter was measured on-line during the protocols. At the entrance to the perfusion channel, a pressure of 45 mmHg was hydrostatically applied.

Cross-correlation analysis

Two-dimensional cross-correlation of subsequent image pairs was performed using a commercial correlation engine (DaVis, version 7.2, LaVision GmbH, Göttingen, Germany) and resulted in a 2D vector field. The pixel resolution of the bright-field microscope images was 2,048 (H) × 1,536 (V). A correlation window size of 256 pixels × 256 pixels (77 µm × 77 µm) was used in the first correlation run and 64 pixels× 64 pixels (19 µm × 19 µm) in the second run.

Numerical simulation of temperature field

Figure S3 shows the geometry considered for the three-dimensional numerical simulation to determine the temperature field inside the microfluidic device, particularly within the artery inspection area. The commercial multiphysics program Comsol (version 6, Comsol, Inc., Burlington, MA) was used. An unstructured mesh was generated using a maximum element scale of 0.5, an element growth rate of 1.75 and a resolution of the narrowest region of 2.5. The resultant mesh consisted of 80,880 points and 411,564 elements. Convective heat loss was considered at all outer surfaces of the microfluidic device, i.e., on the top and bottom, as well as on the side walls. The following boundary conditions were imposed. The heat flux at the top surface was determined by assuming a heat transfer coefficient of 7.84 $W{\cdot}m^{-2}K^{-1}$ and an external temperature of 25˚C. On the bottom surface, the heat flux followed from assuming a heat transfer coefficient of 3.92 $W{\cdot}m^{-2}K^{-1}$ and a temperature of 25˚C. At all side walls, the heat transfer coefficient of 12.34 $W{\cdot}m^{-2}K^{-1}$ and the temperature of 25˚C were used. Similarly to the laboratory experiment, a constant temperature was obtained by controlling the heat that the thermoelectric element (TE) produced with a proportional–integral–derivative (PID) controller. The produced heat flux was expressed as $Q_{TE} = k_P(T - T_{set}) + k_I\int(T - T_{set})dt + k_D\,dT/dt$ with the following parameters: $k_P = 5$ $N{\cdot}mm^{-1}s^{-1}K^{-1}$; $k_i = 0.05$ $N{\cdot}mm^{-1}s^{-2}K^{-1}$; $k_D = 0.15$ $N{\cdot}mm^{-1}K^{-1}$, set-point temperature $T_{set} = 37.5$˚C, and the temperature T measured at the center of the thermistor ("B" in Fig. S3). The heat transfer coefficient was calculated using a standard correlation.[3] The thermal conductivity of PDMS was assumed $0.17W{\cdot}m^{-1}{\cdot}K^{-1}$, the density 0.97 $kg{\cdot}m^{-3}$, and the heat capacity 1.2 $kJ{\cdot}kg^{-1}{\cdot}\,K^{-1}$. All other material properties were selected from the Comsol database (glass $h = 1.2$ $W{\cdot}m^{-1}{\cdot}K^{-1}$, sapphire $h = 32W{\cdot}m^{-1}{\cdot}K^{-1}$). A direct linear solver (Paradiso) was used to obtain the convergent steady-state temperature field during a time-dependent numerical simulation. Convergence was assessed by integrating the heat flux across the bottom surface of the TE element and inspecting temperature at various points in the geometry as indicated in the table below. The obtained values were compared with results from a coarser grid (Mesh 2) with a

Electronic Supplementary Information (ESI):
A microfluidic platform for probing small artery structure and function

Axel Günther, Sanjesh Yasotharan, Andrei Vagaon, Conrad Lochovsky, Sascha Pinto, Jingli Yang, Calvin Lau, Julia Voigtlaender-Bolz, Steffen-Sebastian Bolz

resolution of narrowest regions of 2, resulting in a mesh consisting of 55,134 mesh points and 285,630 elements.

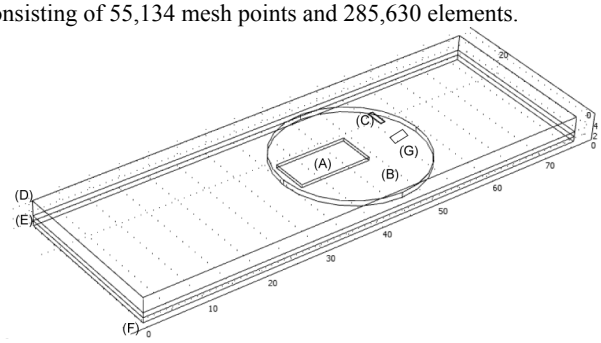

Fig. S3 The figure outlines the geometry used for the numerical simulation of the temperature field within the microfluidic device. The TE element (A) was treated as a heat source with a power output (Q_{TE}) that was determined by a PID controller using the temperature measured at the center of a representation of a thermistor (C). Heater and thermistor are both attached to a 1mm thick with a 25 mm diameter sapphire disk (B). This entire assembly was embedded in PDMS (D and E) and bonded to a flat layer of soda lime glass (F). The artery inspection location is indicated by (G) just above the glass surface.

Calculated properties	**Mesh 1**	**Mesh 2**
Temperature at thermistor	37.50˚C	37.50˚C
Temperature at bottom edge of sapphire disk	37.36˚C	37.36˚C
Heat output of thermoelectric element	0.156 W	0.154 W

Numerical simulation of velocity and concentration fields

A commercial finite element code (Comsol version 6, Comsol, Inc., Burlington, MA) was used to numerically predict the velocity and concentration fields in the vicinity of the artery segment. The mesh was generated using a maximum element size of 15µm, an element growth rate of 1.2 and a resolution of the narrowest region of 5. The resulting unstructured mesh consisted of 65,107 points, 121,371 elements, and a minimum element quality of 0.64.

The following boundary conditions were imposed on the system. At the perfusion inlet, an entrance length was 6 mm was used and a gauge pressure of 58 mmHg applied. The top fixation channels (**E_1** in Fig. 1) were characterized by a gauge pressure of -43 mmHg and an exit length of 13mm. The bottom fixation channels (**E_2** in Fig. 1) were subjected to a gauge pressure of -43 mmHg and an exit channel length of 34 mm. By assuming a uniform channel depth of 150 µm, the superfusion inlet (**B** in Fig. 1) had a volumetric flow rate of 4 mL/h and the entrance length was 138 mm. At the superfusion outlet, the gauge pressure was -6 mmHg and the exit length was 40mm. The pressures were selected such that the simulation accurately matched the hydrostatic pressures used in our experiments. The pressure drops present in the polymer tubes and metal pins leading to and from the chip were therefore estimated by assuming Poiseuille flow in the tubes to calculate the fluidic resistance, and estimates of flow rates in the superfusion and perfusion lines.

A direct linear solver (Paradiso) was used with a relative tolerance of 1.0×10^{-7}. The convergence of the obtained solution was assessed by integrating the calculated fluid velocity across the flow channel at various locations and assuming a uniform microchannel depth of 150µm (table below). These values were compared with results obtained from a courser numerical grid (Mesh 2). Mesh 2 was generated using a maximum element size of 20µm, an element growth rate of 1.2, and a resolution of the narrowest regions of 5. The resulting mesh had 47,400 points, 86,950 elements and a minimum element quality of 0.647. Even though microchannel **D** was blocked, the predicted Reynolds number for the artery perfusion was 0.977 due to leakage through fixation channel **E_2**. The Reynolds number in the narrow region of the superfusion inlet was 9.27. The gauge pressure at artery abluminal side was -3.6 mmHg and the transmural pressure was 49.55 mmHg.

Velocity integrated across flow channel	**Mesh 1 (mL/h)**	**Mesh 2 (mL/h)**
Perfusion inflow rate (Q_A)	3.130	3.130
Perfusion inflow rate at constriction point	3.128	3.127
Superfusion inflow rate (Q_B)	4.000	4.000
Top fixation outflow rate (Q_{E1})	1.715	1.715

Experimental validation of selective small artery perfusion and superfusion

Videos S4-S5 show bright field or fluorescence micrographs of small artery perfusion or superfusion in the inspection section of device I. Video S4 shows perfusion of the artery with clear medium while a stepwise increasing concentration of a fluorescent marker was applied at the outer artery wall. Video S5 shows small artery constriction while a stepwise increasing concentration of phenylephrine was applied on both sides. Videos S6A and S6B correspond to cases where a heterogeneous microenvironment was established at the artery abluminal side. Only one half of the outer artery circumference was selectively labeled using a fluorescent marker. The fluorescent micrographs confirm the marker to be strictly constrained to the side of its application only.

Video S4. Video of clear perfusion stream with fluorescently labelled (Fluorescein) superfusion stream to illustrate rapid change in concentration on artery abluminal side as well as complete separation between fluorescently labelled superfusion and clear perfusing streams. The total superfusion flow rate was kept constant at 4 mL/h while switching between fluorescently

Electronic Supplementary Information (ESI):
A microfluidic platform for probing small artery structure and function

Axel Günther, Sanjesh Yasotharan, Andrei Vagaon, Conrad Lochovsky, Sascha Pinto, Jingli Yang, Calvin Lau, Julia Voigtlaender-Bolz, Steffen-Sebastian Bolz

labelled superfusion stream ($\mathbf{B_1}$) and clear buffer (MOPS) stream ($\mathbf{B_2}$).

Video S5. Video of artery constricting on a chip in response to a stepwise increase of phenylephrine. Transmural pressure of 45 mmHg was applied with total superfusion flowrate at 4mL/h.

Video S6 (A) Video demonstrating isolation of left and right side of organ bath in split chip. Experimental conditions are similar to Video S5. Left half of the abluminal side subjected to a stepwise increasing and subsequently decreasing dye concentration while right side was superfused with non-labelled stream. Video is in real time. (B) Video demonstrating isolation of left and right side of organ bath in split chip. Experimental conditions are similar to Video S5. First, left half and then the right half of the abluminal side were subjected to stepwise increasing dye concentrations. Then the dye concentration was stepwise decreased, first on the left half and then on the right half. Video is in real time.

Supplementary references

1. M. A. Unger, H. P. Chou, T. Thorsen, A. Scherer and S. R. Quake, *Science*, 2000, **288**, 113-116.
2. Y. N. Xia and G. M. Whitesides, *Annual Review of Materials Science*, 1998, **28**, 153-184.
3. Incropera, FP, DeWitt, DP, Fundamentals of Heat and Mass Transfer, 4th Ed., Wiley, New York, p. 493.